Received: 23 February 2023 | Revised: 22 April 2023 | Accepted: 12 May 2023

DOI: 10.1002/biot.202300091

Biotechnology Journal

RESEARCH ARTICLE

Cellulase mediated stress triggers the mutations of oleaginous yeast *Trichosporon cutaneum* with super-large spindle morphology and high lipid accumulation

Qi Liu | **Yuanyuan Li** | **Weiliang Hou** | **Bin Zhang** | **Jie Bao**

State Key Laboratory of Bioreactor Engineering, East China University of Science and Technology, Shanghai, China

Correspondence
Jie Bao and Bin Zhang, State Key Laboratory of Bioreactor Engineering, East China University of Science and Technology, Shanghai 200237, China.
Email: jbao@ecust.edu.cn (JB) and y10190152@mail.ecust.edu.cn (BZ)

Funding information
National Natural Science Foundation of China, Grant/Award Number: 21978083; Science and Technology Committee of Shanghai Municipality, Grant/Award Number: 23YF1409900

Abstract

Accumulation of intracellular lipid bodies in oleaginous yeast cells is highly restricted by their natural intracellular space. Here we show a cellulase mediated adaptive evolution with ultra-centrifugation fractionation of oleaginous yeast *Trichosporon cutaneum* to obtain the favorable cell structure for lipid accumulation. Cellulase was added to the wheat straw hydrolysate during long-term adaptive evolution for disruption of cell wall integrity of *T. cutaneum* cells. The cellulase, together with ultracentrifugation force, triggered multiple mutations and transcriptional expression changes of the functional genes associated with cell wall integrity and lipid synthesis metabolism. The fractionated mutant *T. cutaneum* YY52 demonstrated the heavily weakened cell wall and high lipid accumulation by the super-large expanded spindle cells (two orders of magnitude greater than the parental). A record-high lipid production by *T. cutaneum* YY52 was achieved (55.4 ± 0.5 g L^{-1} from wheat straw and 58.4 ± 0.1 g L^{-1} from corn stover). This study not only obtained an oleaginous yeast strain with industrial application potential for lipid production but also provided a new method for generation of mutant cells with high intracellular metabolite accumulation.

KEYWORDS
cell size, cell wall structure, cellulase, microbial lipid, oleaginous yeast

1 | INTRODUCTION

Microbial lipid production using lignocellulose biomass as carbohydrates feedstock provides the most sustainable lipid supply for production of biodiesel and aviation biofuel.[1,2] Oleaginous yeasts have great potential as microbial cell factories.[3,4] However, the accumulation of intracellular lipid bodies in oleaginous yeast cells is highly restricted by their limited cell morphology.[5,6] To change oleaginous yeast cells into a favorable structure for lipid accumulation, the covalently cross-linked mannoproteins outer layer and the glucan-chitin inner layer of the cell walls should be effectively disrupted.[7–9] We speculated that a weakened glucan-chitin layer should contribute to reduced cell wall rigidity and cell volume expansion.[10–12]

Innovative methods are required besides regular mutations and screening to trigger the mutations toward the favorable lipid accumulation morphology of oleaginous yeast cells. Our recent study demonstrated that ultra-centrifugation force in adaptive evolution acted as a highly effective and strong stress on mutating oleaginous yeast *Trichosporon cutaneum* cells with weaken cell wall.[13] Mild centrifugal force has been used to isolate the lighter, lipid-rich oleaginous yeast mutants based on the floating ability of high lipid content cells.[14,15] When ultra-centrifugation force was increased up to 40,000 g, the ultra-centrifugation force during adaptive evolution played a key role in the generation of extraordinarily large *T. cutaneum* mutants with thinner cell wall.[13] However, the potential of ultra-centrifugation force as the functional stress to trigger the mutations

has reached its physical ceiling. To obtain the new mutant cells with more expanding cell morphology with higher lipid accumulation potential, new stress should be introduced into the adaptive evolution to stimulate essential mutations.

Cellulase enzyme is a multi-complex enzyme catalyzing the hydrolysis of β-glycosidic bonds of β-glucan substrates.[16–18] The proximity of cellulase activities makes it capable of hydrolyzing the yeast cell wall β-glucan and disrupting the cell wall integrity.[19,20] Our previous results showed that the transcriptional levels of the genes related to cell wall degradation such as the exoglucanase gene *Trcu_05082* and the mannosidase gene *Trcu_00855* were significantly up-regulated in the large spindle mutant *T. cutaneum* MP11 with high lipid accumulation.[13] We speculated that the excessive existence of cellulase in long-term adaptive evolution of *T. cutaneum* cells could weaken the cell wall integrity and trigger the cell mutations to weakened cell wall and expansion of cell size.

Here we experimentally investigated the cellulase mediated adaptive evolution with ultra-centrifugation fractionation and the speculation was confirmed. A commercial cellulase cocktail was added at the dosage of 3.4 mg protein mL^{-1} to adaptive evolution cultures of *T. cutaneum* in lignocellulose hydrolysates. The lighter cells were fractionated by ultra-centrifugation force in the two-phase (corn oil-broth) medium and re-inoculated into adaptive evolution cultures. This process gradually changed the cells into an extraordinarily larger volume with elevated intracellular lipid content. The obtained strain *T. cutaneum* YY52 was heritably stable with mutations in the genome-scale. The key genes responsible for cell wall structure and lipid synthesis metabolism were analyzed by genome re-sequencing and transcriptome. This work not only obtained a high lipid-producing strain from lignocellulose feedstock but also provided a practical method for generating mutant cells with high intracellular lipid synthesis.

2 | EXPERIMENTAL SECTION

2.1 | Enzymes and reagents

Cellic CTec 2.0 was purchased from Novozymes (China), Beijing, China. The filter paper units were 203.2 FPU mL^{-1}, the cellobiose activity was 4,900 CBU mL^{-1},[21,22] and the protein concentration was 87.31 mg mL^{-1}.[23]

Yeast extract and peptone were purchased from Oxoid, Hampshire, UK. Glucose and other analytic reagent were purchased from Tianchem, Shanghai, China. Corn oil (the brand Luhua, Shandong, China) was purchased from a local supplier.

2.2 | Microorganisms

The parental oleaginous yeast strain *T. cutaneum* ACCC 20271 was obtained from Agricultural Culture Collection of China (ACCC, Beijing, China) and cultured on yeast extract-peptone-dextrose (YPD) medium or the synthetic medium (60 g L^{-1} of glucose, 1.0 g L^{-1} of yeast extract, 1.0 g L^{-1} of KH_2PO_4, 0.5 g L^{-1} of $MgSO_4.7\ H_2O$ and 0.22 g L^{-1} of $(NH_4)_2SO_4$). The whole genome of *T. cutaneum* ACCC 20271 has been deposited at DDBJ/EMBL/GenBank as the accession of LTAL00000000.[24]

The biodetoxification strain *Amorphotheca resinae* ZN1 (CGMCC 7452) was isolated in our previous study.[25] The pretreated wheat straw or corn stover was biodetoxified by *A. resinae* ZN1 as previously described.[26]

2.3 | Lignocellulose feedstock and its biorefinery processing for clear hydrolysate preparation

Wheat straw was collected from Binzhou city, Shandong province, China in summer 2018. Corn stover was collected from Nanyang city, Henan province, China in spring 2020. The wheat straw contained 32.5% w/w cellulose, 21.2% w/w hemicellulose, and 8.1% w/w ash; the corn stover contained 34.4% w/w cellulose, 23.6% w/w hemicellulose, and 4.3% (w/ w) ash determined by NREL LAP protocols.[27,28]

The raw material was dry acid pretreated according to our previous protocols.[29,30] The pretreated biomass was neutralized to pH 5.5, and then biodetoxified by inoculating *A. resinae* ZN1 to remove the inhibitors (furfural, 5-hydroxymethylfurfural, acetic acid and phenolic aldehydes) according to our previous work.[25,31]

To obtain the clear wheat straw hydrolysate, the dry acid pretreated and biodetoxified wheat straw was enzymatically hydrolyzed at the solids loading of 15% w/w or 30% w/w and the enzyme dosage of 6 mg cellulase protein per gram of dry solid matter. The hydrolysis was conducted in a 5 L fermenter for 48 h at 50°C, 150 rpm. The hydrolysate slurry was centrifuged to remove the insoluble residues and then sterilized at 115°C for 20 min to inactivate cellulase. The obtained clear wheat straw hydrolysate contained 60.1 g L^{-1} of glucose, 15.2 g L^{-1} of xylose, 0.6 g L^{-1} of galactose, 1,7 g L^{-1} of mannose and arabinose, and few phenolic inhibitors (60.21 mg L^{-1} of 4-hydroxybenzaldehyde, 79.62 mg L^{-1} of vanillin and 30.34 mg L^{-1} of syringaldehyde). The nutrients of 1.0 g L^{-1} of KH_2PO_4, 0.5 g L^{-1} of yeast extract, 0.5 g L^{-1} of $MgSO_4{\cdot}7H_2O$ and 0.22 g L^{-1} of $(NH_4)_2SO_4$ were added.

2.4 | Ultra-centrifugation fractionation in adaptive evolution

The parental strain *T. cutaneum* ACCC 20271 was cultured at 30°C, 180 rpm for 4 days in 500 mL flasks containing 50 mL of wheat straw hydrolysate. 15 mL broth was transferred into a 50 mL tube and centrifugated for 3 min at increasing centrifugal force. The upper layer of the broth (5 mL) was pipetted as the seed for the next round of adaptive evolution culture at the inoculum size of 10% v/v. The adaptive evolution was conducted for total 236 days (59 transfer times). The strategy of cellulase addition into culture medium, the centrifugation force of fractionation, and the centrifugation medium was adjusted into four stages as follows

Stage I (from the 1st to the 18th transfers): The cellulase cocktail was added into wheat straw hydrolysate at the dosage of 3.4 mg protein mL^{-1} at every transfer. The centrifugation of the broth was conducted with the increasing centrifugation force from 3000 to 15,000 g (2000-3000 g every three transfers).

Stage II (from the 19th to the 35th transfers): The cellulase was added at the dosage of 3.4 mg protein mL^{-1} at the alternative interval (added in one transfer and did not add in the following transfer). The centrifugation of the broth was conducted with the increasing rate from 18,000 to 40,000 g (2000-5000 g every 2–3 transfers) to the maximum of the centrifuge machine (Beckman J-26XP, Brea, CA).

Stage III (from the 36th to the 46th transfers): The cellulase was added at the dosage of 3.4 mg protein mL^{-1} at the alternative interval (added in one transfer and did not add in the following transfer, same with Stage **I**). At each transfer, 15 mL of corn oil was added to the 15 mL of the broth and mixed in a 50 mL tube before the centrifugation at 40,000 g. After centrifugation, the corn oil layer was in the upper of the broth due to the lower density, and the lighter cells were dispersed in the corn oil layer. 5 mL of corn oil was pipetted as the seed for the next round evolution at the inoculum size of 10% v/v.

Stage IV (from the 47th to the 59th transfers): No cellulase was added to wheat straw hydrolysate in order to obtain the phenotypically stable cells. The centrifugation was conducted without adding corn oil at 40,000 g.

2.5 | Measurement of cell volume and density

The parental *T. cutaneum* ACCC 2020271 cell shape was approximated as a cylinder to calculate the volume (*V*) according to Equation (1)

$$V = \pi\left(\frac{D}{2}\right)^2 h \quad (1)$$

where *D* is the diameter of the cells; h is the length of the cells.

The volume (*V*) of spindle shaped *T. cutaneum* YY52 cell is calculated with reference to the formula for spindle (approximate two cones with joined bottoms) volume according to Equation (2).

$$V = 2 \times \frac{1}{3}\pi\left(\frac{D}{2}\right)^2 h \quad (2)$$

where *D* is the diameter of the cells; *h* is the length of the cells.

Cell length and diameter were analyzed using Nano Measurer software (version 1.2). The average of more than 100 cells were calculated for the measurement of cell volume. Only the mature cells were selected for the calculation of the average volume, while the immature (small) and dividing cells were not be covered.

The cell density is calculated as previously described.[13]

2.6 | Electron microscopy observation

The preparation of field emission scanning electron microscope (FESEM) and transmission electron microscope (TEM) were performed as previously described.[13]

2.7 | Intracellular acetyl-CoA and NADPH measurement

The intracellular acetyl-CoA was measured using Acetyl-CoA Analysis Kit (Solarbio Biotech, Beijing, China). The intracellular NADPH was measured using NADPH Assay Kit (Beyotime Biotech, Shanghai, China).

2.8 | Cell wall components measurement

The contents of glucan and mannan in cell wall were determined as previously described.[32] Chitin in cell wall was measured as previously described.[33]

2.9 | Whole genome re-sequencing and RNA sequencing

Genomic DNA of *T. cutaneum* YY52 was extracted using Yeast Genomic DNA Extraction Kit (Tiangen Biotech, Beijing, China), and re-sequenced using the Illumina NovaSeq platform by Personalbio Co. (Nanjing, China).

Total RNA of two *T. cutaneum* strains (the parental ACCC 20271 and the mutant YY52) cultivated in wheat straw hydrolysate for 12 h were extracted using Trizol reagent (RNAiso Plus, TAKARA, Otsu, Japan). RNA sequencing was conducted using the Illumina HiSeq 2000 system by Personalbio Co. (Nanjing, China).

2.10 | Lipid fermentation

The two *T. cutaneum* strains (the parental ACCC 20271 and the mutant YY52) were cultured in YPD medium at 30°C, 180 rpm for 24 h as the fermentation seeds.

The simultaneous saccharification and lipid co-fermentation (SSCF) using biodetoxified wheat straw or corn stover was conducted in a 5 L bioreactor equipped with a helical ribbon agitator. The biodetoxified materials were pre-hydrolyzed at 30% w/w solids loading with the cellulase dosage of 4 mg protein g^{-1} DM at 50°C for 12 h. The nutrients of 1.0 g L^{-1} KH_2PO_4, 0.5 g L^{-1} yeast extract, 0.5 g L^{-1} $MgSO_4 \cdot 7H_2O$, 0.22 g L^{-1} $(NH_4)_2SO_4$ were added, the *T. cutaneum* seed was then inoculated at the ratio of 10% (v/w). SSCF was carried out at 30°C, 1 vvm of aeration, and 600 rpm stirring. The pH was controlled at 5.0 by automatically adding 4 M HCl.

2.11 | Analytical methods

Glucose and xylose were analyzed using HPLC according to the method described previously.[30] Dry cell mass was measured after centrifugation, washing and drying at 60°C for 24 h till constant weight. Lipid was extracted from the *T. cutaneum* cells using the chloroform-methanol method as previously described.[34,35] The fatty acid composition

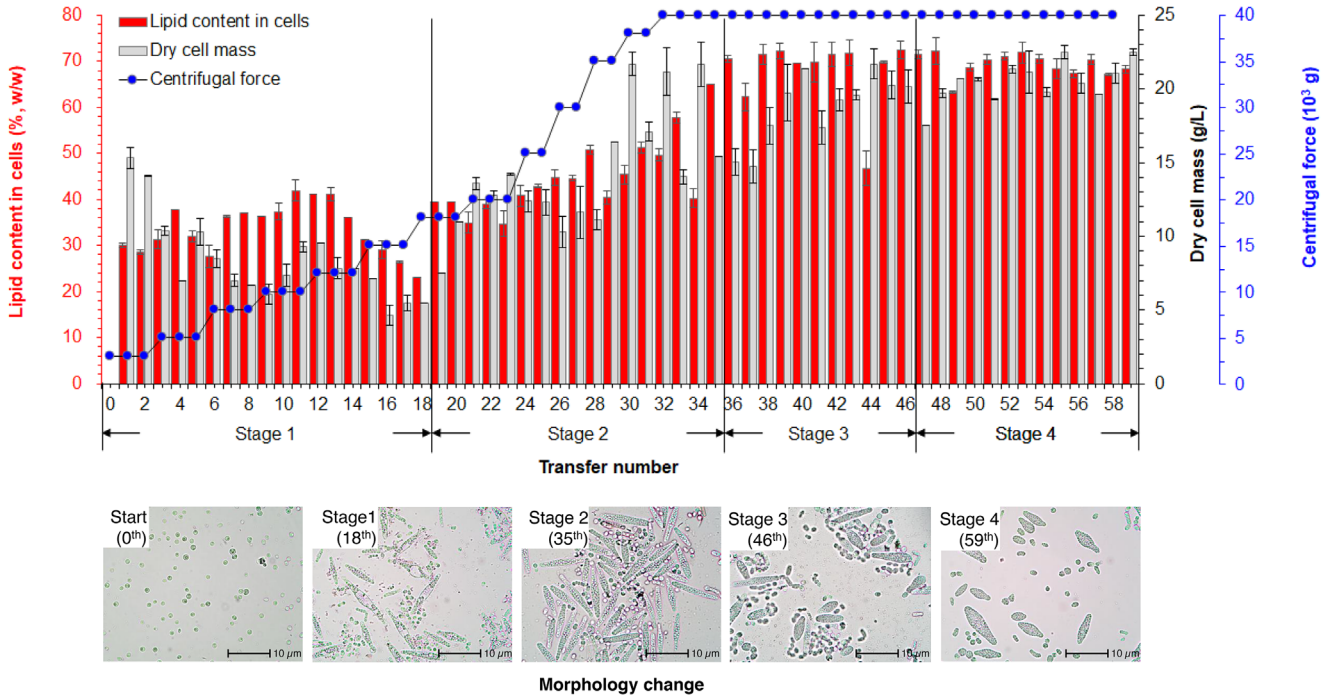

FIGURE 1 Cellulase mediated adaptive evolution with ultra-centrifugation fractionation of *Trichosporon cutaneum* ACCC 20271 cells. Culture conditions and analysis procedures were described in the Methods section ("Microorganisms" and "Ultra-centrifugation fractionation in adaptive evolution").

was determined by gas chromatography-mass spectrometry (GC-MS). Briefly, the GC–MS was operated at the injector temperature of 280°C and 1 mL min^{-1} of nitrogen gas with the temperature gradient of 16°C min^{-1} from 80°C for 3 min till 280°C and held for 8 min.

3 | RESULTS AND DISCUSSION

3.1 | Adaptive evolution of *T. cutaneum* cells under cellulase mediated stress

Excessive commercial cellulase cocktail Cellic CTec2.0 was added at the dosage of 3.4 mg proteins mL^{-1} (approximately three-folds higher than that in general lignocellulose hydrolysis and fermentation) to the adaptive evolution of the parental *T. cutaneum* ACCC 20271 with wheat straw hydrolysate as culture medium (Figure 1). The *T. cutaneum* cells were fractionated with increasing ultra-centrifugation force from 3000 g to 40,000 g in the first 35 transfers (**Stage I** and **Stage II**). In **Stage I** (from the start to the 18^{th} transfer), the cellulase was added to wheat straw hydrolysate at each transfer of adaptive evolution. A significant increase in cell size was observed although the cell growth was still poor and the intracellular lipid bodies were scattered (Figure 1, the 18^{th}).

In **Stage II** (from the 19^{th} to the 36^{th} transfer), the cellulase was added with a cellulase free interval (added in one transfer and not added in the next transfer) to give a rest from the harsh stress of cellulase on cell growth. The dry cell mass increased from 11.1 g L^{-1} (at the 28^{th}) to the ending 15.4 g L^{-1} (at the 35^{th}) and the intracellular lipid content increased from 50.8% to 64.9% due to the relieved cellulase stress on cell growth. The majority of the cells changed into an enlarged rod-like shape and the intracellular lipid bodies occupied nearly the whole intracellular space of the cells (Figure 1, the 35^{th}).

In **Stage III** (from the 36^{th} to the 46^{th} transfer), the ultra-centrifugation fractionation was conducted in the two-phase medium (corn oil-broth) to fractionate the lightest cells on the upper layer of corn oil. The floating force and the viscous force of the cells in the corn oil phase (with the lighter density of ~0.9 g mL^{-1} than water density) were reduced compared to the hydrolysate broth (mainly water with the density close to 1.0 g mL^{-1}) at the maximum centrifugation of 40,000 g (the upper limit of the centrifugal machine). Based on the cell displacement model in the ultra-centrifugation force field,[13] the corn oil medium reduced the floating force on the cells towards the upper direction, thus the lighter cells were fractionated clearly on the surface of corn oil. The intracellular lipid bodies of the cells were further densified with the dry cell mass increased to 22.5 g L^{-1} (at the 46^{th}) and the lipid content increased to approximately 70% w/w (Figure 1, the 46^{th}).

In **Stage IV** (from the 47^{th} to the 59^{th} transfer), cellulase and corn oil were no longer used for verification of the genetic stability of the evolved cells. The cell growth (~23 g L^{-1}), morphology (spindle), and lipid content (~72%, w/w) of the cells were well maintained in this stage (Figures 1 and S1), suggesting a mutant cell might be generated by the cellulase mediated adaptive evolution with ultracentrifugation fractionation. The finally obtained cell was isolated from a single colony on petri dish gel and designated as *T. cutaneum* YY52 (Figure 1, the 59^{th}).

Figure S2 shows the time courses of cell morphology, growth and lipid content of *T. cutaneum* YY52 in wheat straw hydrolysate. Figure S2A indicates that the cells were all in the form of cross-linked long hyphae with an expanded sphere at one end of the cells in the seed culture (0 h); then the cells changed from hyphae form into typical round yeast form and began to accumulate lipid bodies after transferring to wheat straw hydrolysate at 24 h; the cells further changed into rod-like or ellipsoid form at 48 h; finally, the cells grew into expanded spindles with densified lipid bodies at the end of the culture (96 h). Figure S2B indicates that the final dry cell weight of *T. cutaneum* YY52 and the lipid content were 2.5 and 2.7 folds greater (72.5%, w/w) than that of the parental cells, respectively.

3.2 | Cellulase stress in adaptive evolution stress triggered new mutations in genome scale

The phenotype stability of the evolved strain *T. cutaneum* YY52 was evaluated (Figure S3). After six round transfers in YPD medium, the specific phenotypes (morphology and lipid accumulation) of *T. cutaneum* YY52 were found to be well maintained, indicating that the genetic mutations might occur to *T. cutaneum* YY52. The genome of *T. cutaneum* YY52 was re-sequenced and the genomic divergences with its parental *T. cutaneum* ACCC 20271 were illustrated in Supplemental Dataset S1. Totally 1443 single nucleotide polymorphisms (SNPs), 938 small indels (InDels) and 5 copy number variations occurred in *T. cutaneum* YY52, including the cell wall integrity related genes such as *Trcu*_01919 encoding endoglucanase and *Trcu_04438* encoding β-glucan synthesis-associated protein, as well as the lipid synthesis related genes such as *Trcu_02066* encoding citrate synthase and *Trcu_04595* encoding acetyl-CoA carboxylase (Table S1). These genomic mutations confirmed that the genetic stability od *T. cutaneum* YY52 should come from its genomic mutations.

The differential gene expressions between the mutant *T. cutaneum* YY52 and the parental *T. cutaneum* ACCC 20271 were further investigated by comparative transcriptome analysis (Figure S4 and Supplemental Dataset S2). Totally 1722 differentially expressed genes (DEGs) were identified in the threshold criterion of $|\log_2\text{-fold change}| > 1$ and p-value < 0.05, including 935 upregulated and 781 downregulated genes (Figure S4A). The Kyoto Encyclopedia of Genes and Genomes (KEGG) pathway enrichment analysis revealed that more than 60% of the DEGs were involved in metabolism processing (Figure S4B).

On lipid synthesis metabolism, the central carbon metabolism of lipid biosynthesis in *T. cutaneum* YY52 was constructed based on the comparative transcriptome analysis (Figure 2A). Lipid accumulation highly depends on intracellular acetyl-CoA flux, NADPH supply, and synthesis capacity of free fatty acid and triglyceride. The first glance on sugar assimilation pathways showed that the genes involved in glucose and xylose assimilation of *T. cutaneum* YY52 were generally up-regulated. The up-regulated citrate synthase (CS) gene *Trcu*_02066 and the up-regulated ATP-citrate lyase (ACL) gene, as well as the down-regulated aconitase (ACO) gene both facilitated the synthesis of cytosol acetyl-CoA as lipid precursor. A genetic mutation also occurred for the up-regulated gene *Trcu*_02066 (Table S1). The genes associated with NADPH regeneration such as malic enzyme (ME) gene and isocitrate dehydrogenase (IDH) gene showed significant up-regulations. The genes involved in fatty acids/triglyceride synthesis pathway were all up-regulated by 2.5 to 33.4-folds, among which the genetic mutations occurred for acetyl-CoA carboxylase (ACC) *Trcu*_04595 and diacylglycerol acyltransferase (DGAT) *Trcu*_05085 (Table S1). The transcriptional results were confirmed by the experimentally measured intracellular contents of acetyl-CoA (2.8- to 12.2-folds greater than the parental) and NADPH (8.0- to 18.4-folds greater than the parental) (Figure S5).

On cell wall metabolism, the cell wall degradation genes were investigated in *T. cutaneum* YY52. The comparative transcriptome analysis indicates that several glucanase genes responsible for glucan degradation and two mannanase genes responsible for mannan degradation were up-regulated in *T. cutaneum* YY52 (Figure 2B). Among which, the endoglucanase gene *Trcu*_01919 was dramatically up-regulated by 185.8-folds, coincidentally a genetic mutation also occurred in *Trcu*_01919 (Table S1). The genetic mutation and the differential expression of *Trcu*_01919 should be responsible for the formation of a fragile cell wall of *T. cutaneum* YY52.

3.3 | Morphology and structure analysis of *T. cutaneum* cells

The genetic mutation and up-regulated expression responsible for cell wall degradation showed a significantly aggravated cell wall morphology (Figures 3 and 4). The glucan content of *T. cutaneum* YY52 decreased by 91.7% compared with that of the parental strain; the mannan content was reduced by nearly 50%; the chitin content maintained relatively constant (Figure 3A). The main components of yeast cell wall polysaccharides are glucan and mannan. Glucan serves as the main load-bearing polysaccharide that contributes to the rigidity of the cell wall and combines with chitin to form a fibrous scaffold.[12] The reduction of cell wall glucan and mannan contents of the *T. cutaneum* YY52 mutant disrupted the cell wall rigidity, weakened the cell wall and changed the cell size (Figure 3B). The cell volume of *T. cutaneum* YY52 was significantly expanded by approximately two orders of magnitude than that of the parental (5.44×10^{-15} m^3 vs. 9.27×10^{-17} m^3). Correspondingly, the cell density of *T. cutaneum* YY52 (990.6 kg $m^{3\text{-}1}$) was reduced than that of the parental cell (1069.5 kg $m^{3\text{-}1}$) and the fermentation broth density (1010.9 kg $m^{3\text{-}1}$). Compared with the previously obtained *T. cutaneum* MP11, *T. cutaneum* YY52 under the double stresses of cellulase and ultracentrifugation showed the greater reduction of glucan content (Figure 3A), the higher lipid content and the lower cell density (Figure 3B). The results indicated the vital role of cellulase mediated stress in generation of mutations on cell wall structure and morphology.

The cell wall components and microcosmic appearance were further analyzed by means of transmission electron microscopy (TEM)

(A)

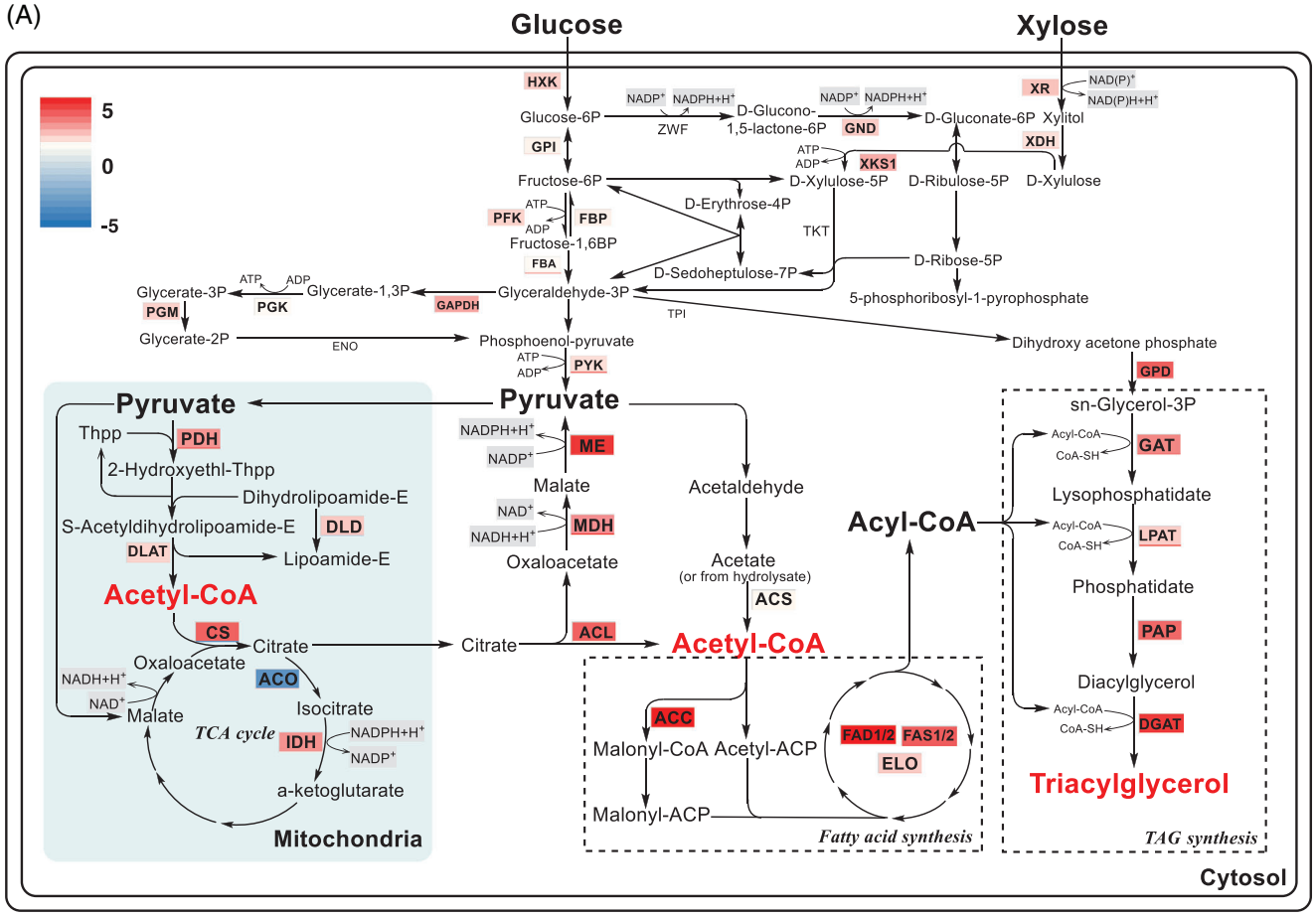

(B)

Gene ID	Annotation	Log_2 Fold change
Glucan		
Trcu_01919	Endoglucanase	7.5
Trcu_05082	Exo-beta-1,3-glucanase	2.0
Trcu_03961	beta-glucosidase	1.4
Trcu_02890	Beta-glucosidase	3.3
Trcu_02915	Beta-glucosidase	4.7
Trcu_03972	Glucosidase	4.0
Mannan		
Trcu_03942	Alpha-mannosidase	2.0
Trcu_00569	mannosyl-oligosaccharide alpha-1,2-mannosidase	1.8

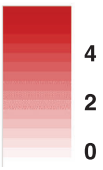

FIGURE 2 Comparative transcriptome analysis of *Trichosporon cutaneum* YY52 compared with the parental. (A) Transcriptional levels of DEGs involved in lipid metabolism. (B) Transcriptional levels of differentially expressed genes (DEGs) involved in cell wall metabolism. The samples were harvested from wheat straw hydrolysate at 24 h, then washed with distilled water and frozen for mRNA extraction. The DEGs are highlighted in bold. The transcriptional levels of DEGs in log2-fold change were represented by color gradations. ACC, acetyl-CoA carboxylase; ACL, ATP-dependent citrate lyase; ACO, aconitase; ACS, acetyl-CoA synthetase; CS, citrate synthase; DGAT, diacylglycerol acyl-transferase; DLAT, dihydrolipoamide acetyltransferase; DLD, dihydrolipoamide dehydrogenase; ELO, fatty acid elongase; ENO, enolase; FAD1/2, delta-9 (12) fatty acid desaturase; FAS1/2, fatty-acid synthase complex protein 1/2; FBA, fructose-bisphosphate aldolase; FBP, fructose-1,6-bisphosphatase; GADPH, glyceraldehyde 3-phosphate dehydrogenase; GAT, glycerol-3-phosphate acyltransferase; GND, phosphogluconate dehydrogenase; GPD, Glycerol-3-phosphate dehydrogenase; GPI, glucose-6-phosphate isomerase; HXK, hexokinase; IDH, isocitrate dehydrogenase; LPAT, lysophosphatidic acid acyltransferase; MDH, malate dehydrogenase; ME, malic enzyme; PAP, phosphatidic acid phosphatase; PDH, pyruvate dehydrogenase; PFK, 6-phosphofructokinase; PGK, phosphoglycerate kinase; PGM, phosphoglycerate mutase; PYK, pyruvate kinase; TKT, transketolase; XDH, xylitol dehydrogenase; XKS1, xylulokinase; XR, xylulokinase; ZWF, glucose-6-phosphate dehydrogenase.

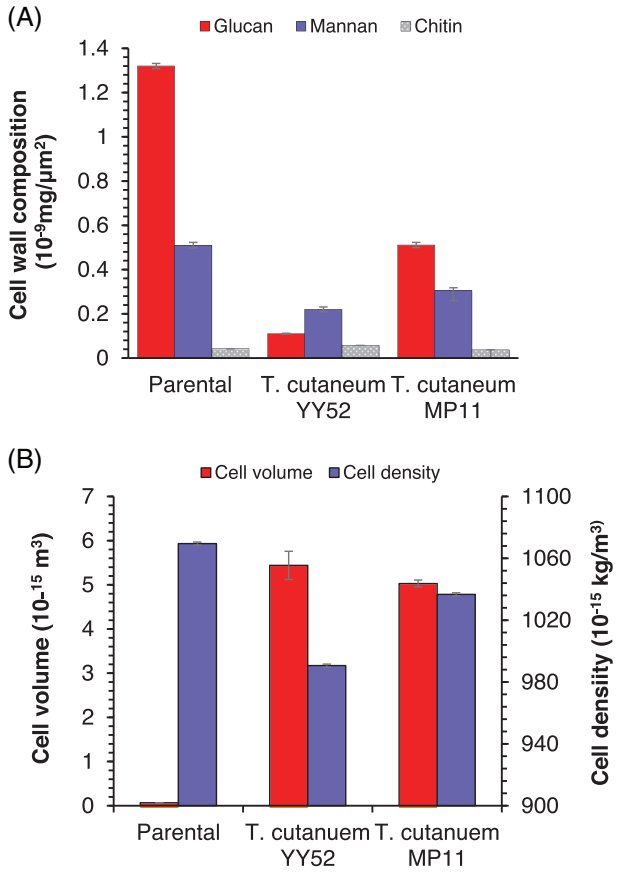

FIGURE 3 Cell wall compositions, cell volume and density of parental, *Trichosporon cutaneum* YY52 and *T. cutaneum* MP11. (A) Cell wall composition. (B) Cell volume and density. The cells used for measurement were cultivated in synthetic medium at 30°C and 180 rpm incubation rate for 96 h.

and field emission scanning electron microscopy images (FESEM) (Figure 4). The TEM images on the cross sections of the cells (Figure 4A) reveal that lipid bodies occupied almost the whole intracellular space of *T. cutaneum* YY52, and the cell wall (glucan-chitin layer, and mannan layer) of *T. cutaneum* YY52 was much thinner than that of the parental cell. The dramatic reduction of glucan content should be responsible for the disruption of cell wall integrity and enable the expansion of cell volume. On the contrary, the slippage (the narrow bright space) between the cytoplasm and cell wall of the parental cell occurred when the cells were sectioned for TEM because of the greater thickness of the cell wall (Figure 4A). The FESEM images reveal that *T. cutaneum* YY52 cells were in the extremely large spindle shape (Figure 4B) and vulnerable to mechanical stress, which might facilitate the extraction of intracellular lipid. Cell wall integrity change had been investigated by secreting cell wall-degrading enzymes for lipid extraction process. Liang et al. (2023) reported that the weakened cell wall strength facilitated lipid extraction of an oleaginous yeast *R. toruloides* NP11 by secretory expression of β-glucomannanase gene MAN5C.[36] Heshof et al. (2020) reported that a co-culture of tow oleaginous yeasts *Schwanniomvces occidentalis* and *Trichoderma harzianum*, and *S. occidentalis* was fed to *T. harzianum* to produce enzymes to degrade the cell wall of *S. occidentalis* for lipid extraction.[37] The cellulase could hydrolyze the yeast cell wall β-glucan and disrupt the cell wall integrity.[19,20] In this study, the mutant *T. cutaneum* strain YY52 with weakened cell wall and extremely expanded cell size obtained by the cellulase mediated adaptive evolution with ultracentrifugation fractionation. The easily broken property of the cells might facilitate the extraction of intracellular lipid from culture broth in practical applications.[38]

3.4 | Evaluations of fermentability and cellulosic lipid production of *T. cutaneum* YY52

The weaken cell wall structure, larger intracellular space of *T. cutaneum* YY52 are favorable for lipid biosynthesis and accumulation. Lipid fermentability of *T. cutaneum* YY52 using lignocellulose feedstock was evaluated by simultaneous saccharification and co-fermentation (SSCF) of the pretreated and biodetoxified wheat straw or corn stover at 30% w/w solids loading (Figure 5). The lipid production from wheat straw reached 55.4 ± 0.5 g L^{-1} at 96 h, or 6.1% v/v in volumetric percentage, approximately 7.2-folds greater than that of the parental *T. cutaneum* ACCC 20271. In our previous study, a mutant strain *T. cutaneum* strain MP11 was obtained by adaptive evolution with ultra-centrifugation fractionation without additional stress. In this study, *T. cutaneum* YY52 was obtained with additional cellulase stress during adaptive evolution with ultra-centrifugation fractionation. Comparing with *T. cutaneum* MP11, *T. cutaneum* YY52 exhibited 1.6-fold higher lipid production and productivity using wheat straw as feedstock.[13] Both glucose and xylose were completely utilized by *T. cutaneum* YY52, comparing with the substantial residual sugars by the parental strain (total 123.4 g L^{-1} of glucose and xylose). The consumption of other three non-glucose sugars (arabinose, galactose, and mannose) was not measured, but we speculate that these sugars were also completely assimilated by *T. cutaneum* YY52, similar to the previously obtained *T. cutaneum* MP11.[13] The lipid yield was 0.19 g g^{-1} biodetoxified wheat straw based on dry weight. Due to the dry weight loss (~8%, w/w) during pretreatment and biodetoxification, corresponding to 5.7 ton of dry wheat straw can be used for production of one ton of microbial lipid (without considering the loss in recovery step)

When corn stover was used as feedstock, the lipid production was 58.4 ± 0.1 g L^{-1} at 120 h, or 6.5% v/v in volumetric percentage, approximately 5.7-fold greater than that of the parental strain (7.7 g L^{-1}). Corn stover generated more inhibitory compounds than wheat straw under the same pretreatment conditions, thus a longer fermentation time was required (120 h of corn stover vs. 96 h of wheat straw). The lipid yield was 0.20 g g^{-1} biodetoxified corn stover based on dry weight by *T. cutaneum* YY52, equivalent to 5.4 tons of dry corn stover was used for production of one ton of microbial lipid, similar to wheat straw feedstock.

The lipid production by various oleaginous microorganisms using lignocellulose as feedstocks are summarized in Table 1. Table 1A shows that *T. cutaneum* YY52 achieved record-high lipid production

TABLE 1 Lipid fermentation performance of oleaginous microorganisms using lignocellulose hydrolysates.

A Lipid production

Strains	Feedstocks	Biorefining methods	Titer (g/L)	Productivity (g/L/d)	Content (%)	Sources
Trichosporon cutaneum YY52	Corn stover	Dry acid pretreatment, biodetoxification, SSF	58.4	11.7	71.3*	This study
Trichosporon cutaneum YY52	Wheat straw	Dry acid pretreatment, biodetoxification, SSF	55.4	13.9	72.5*	This study
Trichosporon cutaneum MP11	Wheat straw	Dry acid pretreatment, biodetoxification, SSF	34.4	8.6	67.8*	[13]
Trichosporon cutaneum ACCC 20271	Corn stover	Dry acid pretreatment, biodetoxification, SSF	8.1	1.1	27.0*	[42]
Trichosporon cutaneum CH002	Corncob	Dilute acid hydrolysate, overliming, SHF	10.4	2.1	33.5	[43]
Trichosporon dermatis CH007	Corncob	Dilute acid pretreatment, water washing, SHF	9.8	1.4	36.0	[44]
Chlorococcum humicola UCDFST 10–1004	Corn stover	Ammonia fiber expansion pretreatment, SHF	15.5	1.2	27	[38]
Cryptococcus curvatus ATCC 20509	Corn stover	Alkali pretreatment, water washing, SSELF	7.4	2.5	59.9	[39]
Cryptococcus curvalus ATCC 20509	Wheat straw	Dilute acid hydrolysate, overliming, SHF	5.8	1	33.5	[36]
Lipomyces kononenkoae Y-7042	Corn stover	Ammonia fiber expansion pretreatment, SHF	28.1	4.3	59.0	[40]
Mortierella isabelline M2	Rice straw	NaOH pretreatment, SHF	23.4	2.9	55.7	[45]
Mortierella isabellina NRRL 1757	Wheat straw	Dilute acid hydrolysate, SHF	4.4	0.7	36.3	[37]
Rhodotorula graminis DBVPG 4620	Corn stover	Dilute acid pretreatment, SHF	16.3	5.4	40.0	[41]

B Fatty acid composition

Strains	Feedstocks	Palmitic acid (C16:0)	Palmitoleic acid (C16:1)	Stearic acid (C18:0)	Oleic acid (C18:1)	Linoleic acid (C18:2)	Others	Sources
Trichosporon cutaneum YY52	Wheat straw	28.2	1.4	19.7	40.7	2.2	2.3	This study
Trichosporon cutaneum MP11	Wheat straw	31.0	2.2	18.2	41.6	1.5	5.5	[13]
Trichosporon cutaneum ACCC 20271	Corn stover	19.4	10.7	6.0	42.1	4.3	17.5	[42]
Cryptococcus curvalus ACCC 20509	Corn stover	25.3	0.6	14.6	51.1	5.9	0.6	[39]
Mortierella isabellina ACCC 42613	Corn stover	24.6	2.5	3.8	54.5	10.6	4.1	[46]
Rhodotorula graminis DBVPG 4620	Corn stover	20.5	–	7.2	42.1	17.2	13.0	[41]
Mortierella isabellina NRRL 1757	Wheat straw	26.2	1.5	6.8	49.9	9.0	6.4	[37]
Cryptococcus curvalus ACCC 20509	Wheat straw	25.9	–	15.2	47.7	6.4	4.8	[36]
Trichosporon cutaneum CH002	Corncob	28.0	–	16.5	46.6	4.9	4.0	[43]
Trichosporon dermatis CH007	Corncob	27.7	–	13.6	43.4	10	5.3	[44]
Candida tropicalis X37	Palm empty fruit bunches	26.2	4.8	9.5	24.7	18.5	16.3	[47]

*The measurement of lipid content was carried out in clear hydrolysate culture after the solids were removed by centrifugation. SSF, simultaneous saccharification and fermentation. SHF, separate hydrolysis and fermentation. SSELF, simultaneous saccharification and enhanced lipid production.

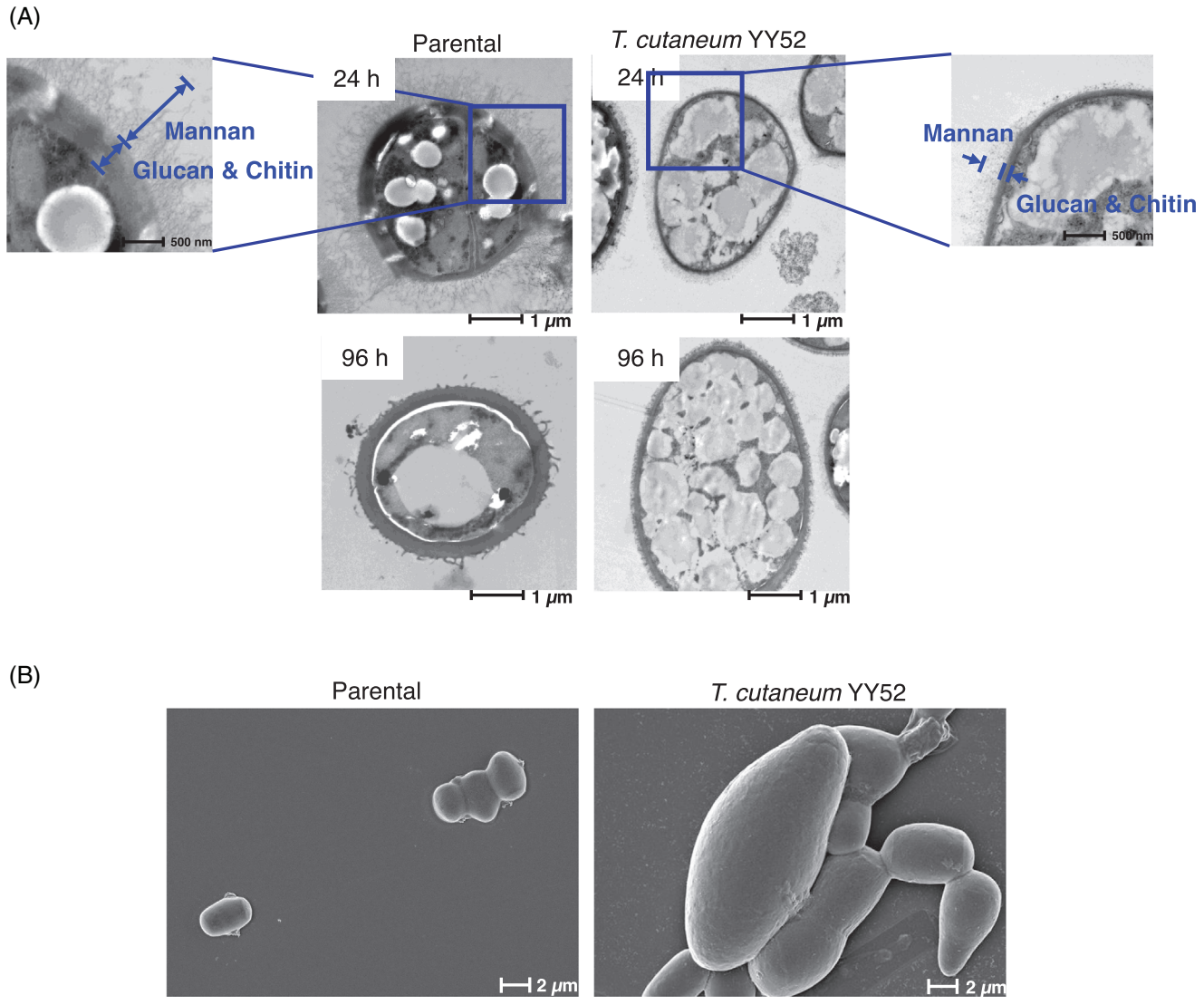

FIGURE 4 Microscale observation of the cell morphology and structure of *Trichosporon cutaneum* cells after cellulase mediated adaptive evolution with ultra-centrifugation fractionation. (A) Transmission Electron Microscope (TEM) images. The TEM images of the parental at 24 h were cited from our previous study[13] due to the same strain and culture conditions. (B) Field emission scanning electron microscope (FESEM) images. The cells used for taking micrograph were cultivated in synthetic medium at 30°C and 180 rpm incubation rate for 96 h.

(55.4 g L^{-1} and 72.5% using wheat straw, 58.4 g L^{-1} and 71.3% using corn stover). As the comparisons, *C. curvalus* ACCC 20509 produced 5.8 g L^{-1} of lipid from wheat straw with lipid content of 36.3%[39]; *M. Isabellina* NRRL 1757 produced 4.4 g L^{-1} of lipid from wheat straw with lipid content of 36.6%[40]; the lipid production and lipid contents from corn stover by *C. humicola* UCDFST 10–1004, *C. curvalus* ATCC 20509, *L. kononenkoae* Y-7042 and *R. graminis* DBVPG 4620 were 15.5 g L^{-1} and 27.0%, 7.4 g L^{-1} and 59.9%, 28.1 g L^{-1} and 59.0%, 16.3 g L^{-1} and 40.0%, respectively.[31–44] The lipid production by *T. cutaneum* YY52 was also 61% higher than that of the previously obtained *T. cutaneum* MP11 mutant by ultra-centrifugation fractionation (without cellulase mediated stress during adaptive evolution).[13] Table 1B shows the fatty acid compositions of cellulosic lipids by various oleaginous microorganisms. The fatty acid compositions of lipid produced by *T. cutaneum* YY52 were essentially the same with that of the commonly used microbial lipid and vegetable oil, suggesting the high potentials on production of aviation fuels, biodiesel, as well as various food and nutrition products.

4 | CONCLUSION

A cellulase mediated adaptive evolution with ultra-centrifugation fractionation generated a mutant *T. cutaneum* YY52 with significantly expanded cell size and improved lipid accumulation. *T. cutaneum* YY52 showed a high genetic stability with weakened cell wall, highly expanded spindle morphology (two orders of magnitude greater than the parental), and high intracellular lipid content (2.7-fold greater

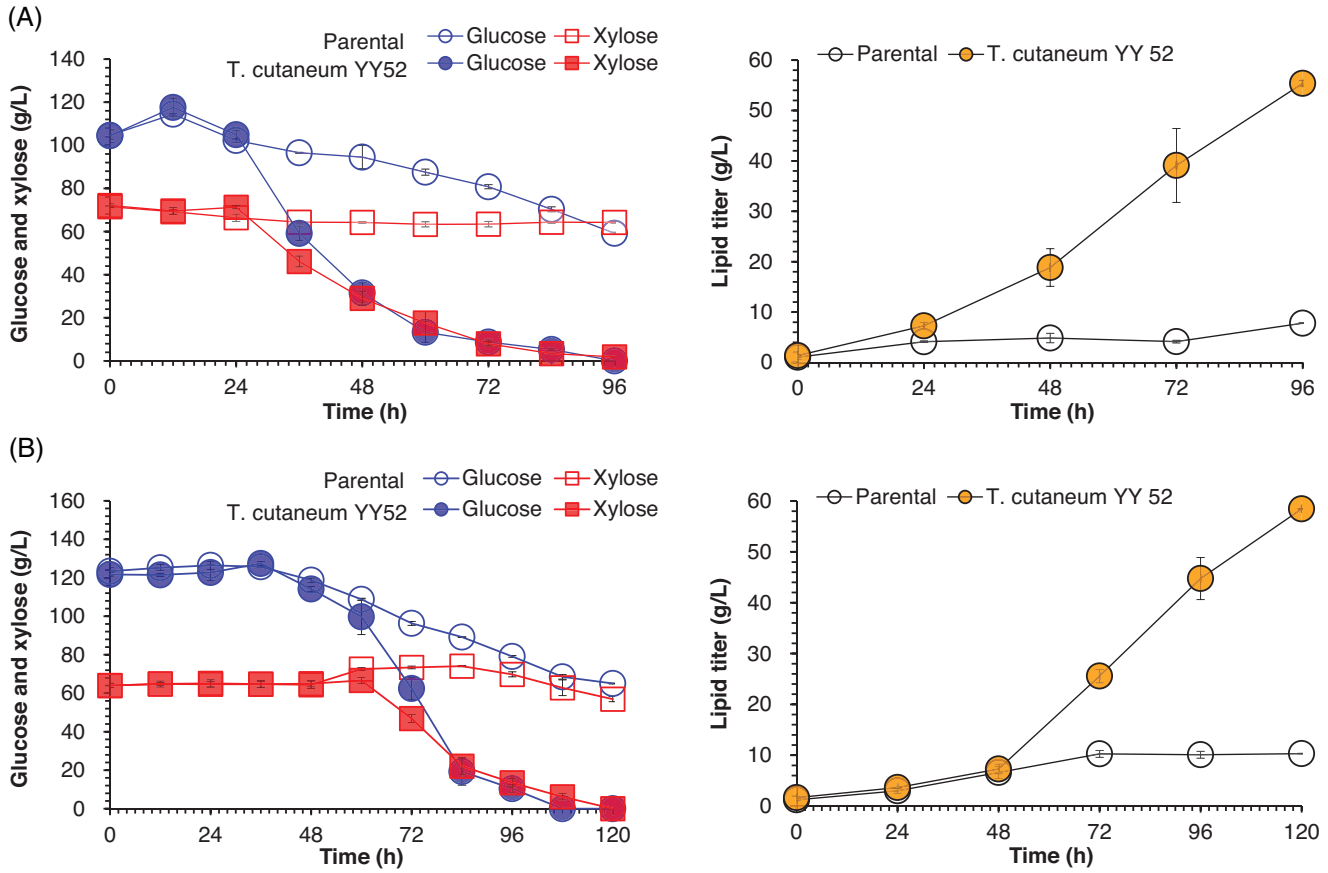

FIGURE 5 Simultaneous saccharification and co-fermentation (SSCF) of wheat straw (A) and corn stover (B) by *Trichosporon cutaneum* YY52. Wheat straw and corn stover were dry acid pretreated, biodetoxified, pre-hydrolyzed and SSCF conducted under 30% w/w solids loading.

than the parental). Whole-genome re-sequencing and transcriptome revealed that the genetic mutation and transcriptional up-regulation of the genes associated with cell wall degradation and lipid synthesis were probably responsible for high lipid accumulation in *T. cutaneum* YY52. A record high lipid production of 55.4 ± 0.5 g L^{-1} or 58.4 ± 0.1 g L^{-1} was obtained from wheat straw or corn stover by SSCF.

AUTHOR CONTRIBUTIONS

Jie Bao and Bin Zhang conceived the study. Weiliang Hou and Jie Bao proposed the idea; Qi Liu and Yuanyuan Li performed the microbial experiments. Qi Liu performed the molecular biology experiments. Yuan-Yuan Li performed the fermentation experiments. Qi Liu, Yuanyuan Li, Weiliang Hou and Bin Zhang performed the data analyses. Qi Liu, Yuanyuan Li and Jie Bao drafted the manuscript. All the authors edited and approved the manuscript.

ACKNOWLEDGMENTS

This research was supported by the National Natural Science Foundation of China (21978083); the Yangfan Project of Science and Technology Committee of Shanghai Municipality (23YF1409900).

CONFLICT OF INTEREST STATEMENT

The authors declare that there is no conflict of interest.

DATA AVAILABILITY STATEMENT

Whole genome re-sequencing and transcriptome data are showed in Supplemental dataset S1 and S2, respectively. All other supporting data are available from the corresponding author on request.

REFERENCES

1. Papadaki, A., Mallouchos, A., Efthymiou, M. N., Gardeli, C., Kopsahelis, N., Aguieiras, E. C., Freire, D. M., Papanikolaou, S., & Koutinas, A. A. (2017). Production of wax esters via microbial oil synthesis from food industry waste and by-product streams. *Bioresource Technology*, *245*, 274–282.
2. Shields-Menard, S. A., Amirsadeghi, M., French, W. T., & Boopathy, R. (2018). A review on microbial lipids as a potential biofuel. *Bioresource Technology*, *259*, 451–460.
3. Sitepu, I. R., Garay, L. A., Sestric, R., Levin, D., Block, D. E., German, J. B., & Boundy-Mills, K. L. (2014). Oleaginous yeasts for biodiesel: Current and future trends in biology and production. *Biotechnology Advances*, *32*, 1336–1360.
4. Vasconcelos, B., Teixeira, J. C., Dragone, G., & Teixeira, J. A. (2019). Oleaginous yeasts for sustainable lipid production—From biodiesel to surf boards, a wide range of "green" applications. *Applied Microbiology and Biotechnology*, *103*, 3651–3667.
5. Timoumi, A., Guillouet, S. E., Molina-Jouve, C., Fillaudeau, L., & Gorret, N. (2018). Impacts of environmental conditions on product formation and morphology of *Yarrowia lipolytica*. *Applied Microbiology and Biotechnology*, *102*, 3831–3848.

6. Shimizu, C., Araki, S., Kuroda, H., Takashio, M., & Shinotsuka, K. (2001). Yeast cellular size and metabolism in relation to the flavor and flavor stability of beer. *Journal of the American Society of Brewing Chemists*, *59*, 122–129.
7. Depree, J., Emerson, G. W., & Sullivan, P. A. (1993). The cell wall of the oleaginous yeast *Trichosporon cutaneum*. *Journal of General Microbiolog*, *139*, 2123–2133.
8. Vega, R., & Domínguez, A. (1986). Cell wall composition of the yeast and mycelial forms of *Yarrowia lipolytica*. *Archives of Microbiology*, *144*, 124–30.
9. Kollar, R., Reinhold, B. B., Petrakova, E., Yeh, H. J., Ashwell, G., Drgonova, J., Kapteyn, J. C., Klis, F. M., & Cabib, E. (1997). Architecture of the yeast cell wall. *Journal of Biological Chemistry*, *272*, 7762–17775.
10. Klis, F. M., Boorsma, A., & De Groot, P. W. (2006). Cell wall construction in *Saccharomyces cerevisiae*. *Yeast*, *23*, 85–202.
11. Orlean, P. (2012). Architecture and biosynthesis of the *Saccharomyces cerevisiae* cell wall. *Genetics*, *192*, 775–818.
12. Cabib, E., Roh, D. H., Schmidt, M., Crotti, L. B, & Varma, A. (2001). The yeast cell wall and septum as paradigms of cell growth and morphogenesis. *Journal of Biological Chemistry*, *276*, 19679.
13. Liu, Q., Lu, M., Jin, C., Hou, W., Zhao, L., & Bao, J. (2022). Ultracentrifugation force in adaptive evolution changes the cell structure of oleaginous yeast *Trichosporon cutaneum* into a favorable space for lipid accumulation. *Biotechnology & Bioengineering*, *119*, 1509–1521.
14. Liu, L., Pan, A., Spofford, C., Zhou, N., & Alper, H. S. (2015). An evolutionary metabolic engineering approach for enhancing lipogenesis in *Yarrowia lipolytica*. *Metabolic Engineering*, *29*, 36–45.
15. Yamazaki, H., Kobayashi, S., Ebina, S., Abe, S., & Takaku, H. (2019). Highly selective isolation and characterization of *lipomyces starkeyi* mutants with increased production of triacylglycerol. *Applied Microbiology and Biotechnology*, *103*, 6297–6308.
16. Murao, S., Yamamoto, R., & Arai, M. (1976). Isolation and identification of red yeast cell wall lytic enzyme producing microorganism. *Agricultural and Biological Chemistry*, *40*, 23–6.
17. Ryu, D., & Mandels, M. (1980). Cellulases: Biosynthesis and applications. *Enzyme and Microbial Technology*, *2*, 91–102.
18. Beldman, G., Leeuwen, M. F. S., Rombouts, F. M., & Voragen, F. G. (1985). The cellulase of Trichoderma viride. Purification, characterization and comparison of all detectable endoglucanases, exoglucanases and beta-glucosidases. *European Journal of Biochemistry*, *146*, 301–308.
19. Phaff, H. J. (1977). Enzymatic yeast cell wall degradation. *Advances in Chemistry Series*, *160*, 240–282.
20. Peitersen, N. (1975). Cellulase and protein production from mixed cultures of *Trichoderma viride* and a yeast. *Biotechnology & Bioengineering*, *17*, 1291–1299.
21. Ghose, T. K. (1987). Measurement of cellulase activities. *Pure and Applied Chemistry*, *59*, 257–268.
22. Adney, B., & Baker, J. (1996). Measurement of cellulase activities. Laboratory Analytical Procedure No. 006. *National Renewable Energy Laboratory*.
23. Bradford, M. M. (1976). A rapid and sensitive method for the quantitation of microgram quantities of protein utilizing the principle of protein-dye binding. *Analytical Biochemistry*, *72*, 248–254.
24. Wang, J., Gao, Q., & Bao, J. (2016). Genome sequence of *Trichosporon cutaneum* ACCC 20271: An oleaginous yeast with excellent lignocellulose derived inhibitor tolerance. *Journal of Biotechnology*, *228*, 50–51.
25. Zhang, J., Zhu, Z., Wang, X., Wang, N., & Bao, J. (2010). Biodetoxification of toxins generated from lignocellulose pretreatment using a newly isolated fungus, *Amorphotheca resinae* ZN1, and the consequent ethanol fermentation. *Biotechnology for Biofuels*, *3*, 26.
26. Yi, X., Gao, Q., Zhang, L., Wang, X., He, Y., Hu, F., Zhang, J., Zou, G., Yang, S., Zhou, Z., & Bao, J. (2019). Heterozygous diploid structure of *Amorphotheca resinae* ZN1 contributes efficient biodetoxification on solid pretreated corn stover. *Biotechnology for Biofuels*, *12*, 126.
27. Sluiter, A., Hames, B., Ruiz, R., & Scarlata, C. (2008). Determination of sugars, byproducts, and degradation products in liquid fraction process samples. NREL/TP-510-42623. *National Renewable Energy Laboratory*.
28. Sluiter, A., Hames, B., Scarlata, C., Sluiter, J., & Templeton, D. (2012). Determination of structural carbohydrates and lignin in biomass national renewable. NREL/TP-510-42618. *National Renewable Energy Laboratory*.
29. He, Y., Zhang, J., & Bao, J. (2014). Dry dilute acid pretreatment by co-currently feeding of corn stover feedstock and dilute acid solution without impregnation. *Bioresource Technology*, *158*, 360–364.
30. Zhang, J., Wang, X., Chu, D., He, Y., & Bao, J. (2011). Dry pretreatment of lignocellulose with extremely low steam and water usage for bioethanol production. *Bioresource Technology*, *102*, 4480–4488.
31. He, Y., Zhang, J., & Bao, J. (2016). Acceleration of biodetoxification on dilute acid pretreated lignocellulose feedstock by aeration and the consequent ethanol fermentation evaluation. *Biotechnology for Biofuels*, *9*, 19.
32. Manners, D. J., Masson, A. J., & Patterson, J. C. (1973). The structure of a β-(1→3)-d-glucan from yeast cell walls. *Biochemical Journal*, *135*, 19–30.
33. Domer, J. E. (1971). Monosaccharide and chitin content of cell walls of *Histoplasma capsulatum* and *Blastomyces dermatitidis*. *Journal of Bacteriology*, *107*, 870–877.
34. Morrison, W. R., & Smith, L. M. (1964). Preparation of fatty acid methyl esters and dimethylacetals from lipids with boron fluoride–methanol. *Journal of Lipid Research*, *5*, 600–608.
35. Chen, X., Li, Z., Zhang, X., Hu, F., Ryu, D., & Bao, J. (2009). Screening of oleaginous yeast strains tolerant to lignocellulose degradation compounds. *Applied Biochemistry and Biotechnology*, *159*, 591.
36. Liang, S., Zhang, Y., Lyu, L., Wang, S., & Zhao, Z K. (2023). Secretory expression of β-1,3-glucomannanase in the oleaginous yeast Rhodosporidium toruloides for improved lipid extraction. *Bioresource and Bioprocessing*, *10*, 16.
37. Heshof, R., Visscher, B., van de Zilver, E., van de Vondervoort, R., van Keulen, F., Delahaijie, R. J. B. M., & Wind, R. D. (2020). Production of tailor-made enzymes to facilitate lipid extraction from the oleaginous yeast Schwanniomyces occidentalis. *AMB Express*, *10*, 41.
38. Khot, M., Raut, G., Ghosh, D., Alarcón-Vivero, M., Contreras, D., & Ravikumar, A. (2019). Lipid recovery from oleaginous yeasts: Perspectives and challenges for industrial applications. *Fuel*, *259*, 116292.
39. Yu, X., Zheng, Y., Dorgan, K. M., & Chen, S. (2011). Oil production by oleaginous yeasts using the hydrolysate from pretreatment of wheat straw with dilute sulfuric acid. *Bioresource Technology*, *102*, 6134–6140.
40. Zeng, J., Zheng, Y., Yu, X., Yu, L., Gao, D., & Chen, S. (2013). Lignocellulosic biomass as a carbohydrate source for lipid production by *Mortierella isabellina*. *Bioresource Technology*, *128*, 385–391.
41. Sitepu, I. R., Jin, M., Fernandez, J. E., da Costa, S. L., Balan, V., & Boundy-Mills, K. L. (2014). Identification of oleaginous yeast strains able to accumulate high intracellular lipids when cultivated in alkaline pretreated corn stover. *Applied Microbiology and Biotechnology*, *98*, 7645–7657.
42. Gong, Z., Shen, H., Yang, X., Wang, Q., Xie, H., & Zhao, Z. K. (2013). Efficient conversion of biomass into lipids by using the simultaneous saccharification and enhanced lipid production process. *Biotechnology for Biofuels*, *6*, 36.
43. Slininger, P. J., Dien, B. S., Kurtzman, C. P., Moser, B. R., Bakota, E. L., Thompson, S. R., O'Bryan, P. J., Cotta, M. A., Balan, V., Jin, M., Sousa Lda, C., & Dal, B. E. (2016). Comparative lipid production by oleaginous yeasts in hydrolyzates of lignocellulosic biomass and process strategy for high titers. *Biotechnology & Bioengineering*, *113*, 1676–1690.

44. Galafassi, S., Cucchetti, D., Pizza, F., Franzosi, G., Bianchi, D., & Compagno, C. (2012). Lipid production for second generation biodiesel by the oleaginous yeast *Rhodotorula graminis*. *Bioresource Technology*, *111*, 398–403.
45. Zhao, C., Xie, B., Zhao, R., & Fang, H. (2019). Microbial oil production by *Mortierella isabellina* from sodium hydroxide pretreated rice straw degraded by three-stage enzymatic hydrolysis in the context of on-site cellulase production. *Renewable Energy*, *130*, 281–289.
46. Ruan, Z., Zanotti, M., Wang, X., Ducey, C., & Liu, Y. (2012). Evaluation of lipid accumulation from lignocellulosic sugars by *Mortierella isabellina* for biodiesel production. *Bioresource Technology*, *110*, 198–205.
47. Tampitak, S., Louhasakul, Y., Cheirsilp, B., & Prasertsan, P. (2015). Lipid production from hemicellulose and holocellulose hydrolysate of palm empty fruit bunches by newly isolated oleaginous yeasts. *Applied Biochemistry and Biotechnology*, *176*, 1801–1814.

SUPPORTING INFORMATION

Additional supporting information can be found online in the Supporting Information section at the end of this article.

How to cite this article: Liu, Q., Li, Y., Hou, W., Zhang, B., & Bao, J. (2023). Cellulase mediated stress triggers the mutations of oleaginous yeast *Trichosporon cutaneum* with super-large spindle morphology and high lipid accumulation. *Biotechnology Journal*, e2300091. https://doi.org/10.1002/biot.202300091